

Retrieval and validation of sea surface winds from calibrated RADARSAT ScanSAR images

Xiaofeng Li¹, W. G. Pichel¹, F. Monaldo², C. Wackerman³, R. Beal², P. Clemente-Colón¹, and K. S. Friedman¹

¹NOAA/NESDIS, E/RA3, Room 102 WWBG, 5200 Auth Road,
Camp Springs, MD 20746-4304, USA

Tel: (301)763-8177; Fax: (301)763-8020; Email: xiaofeng.li@noaa.gov

²The Johns Hopkins University Applied Physics Laboratory, Laurel, MD, 20723-6099, USA

³ERIM International, Inc., Ann Arbor, MI 48113-4008, USA

ABSTRACT

Two SAR ocean surface wind retrieval procedures have been developed by The Johns Hopkins University Applied Physics Laboratory (APL procedure) and ERIM International Inc. (ERIM procedure). The APL procedure estimates the SAR wind direction from temporally coincident meteorological model output, and then a SAR wind speed image is computed from the SAR radar cross section (RCS) measurements using the CMOD4 algorithm modified for HH polarization. The ERIM procedure first estimates the wind direction from wind-aligned feature in the SAR image and then estimates the wind speed in a manner similar to the APL model. The wind vector retrieved from the ERIM model has 180 degree wind direction ambiguity.

The APL procedure winds were compared with meteorological model winds, and the RMS error is about 3.49m/s. The ERIM model winds were compared with buoy winds and the RMS error in wind direction was about 31 degrees. The RMS error in wind speed was about 3.5 m/s.

1. INTRODUCTION

The retrieval of sea surface wind speed from high-resolution, wide-swath SAR images has been a focus of study in the SAR research community for the past few years. A research and development program at NOAA/NESDIS with partners in government, academia, and industry has endeavored to develop coastal ocean SAR applications, in particular wind measurement and hard target detection. These applications are being prepared for a preoperational demonstration in Alaska (the Alaska SAR Demonstration) starting in the fall of 1999. The primary data source will be quick-look, wide-swath SAR (i.e., ScanSAR Wide B) imagery processed at the Alaska SAR Facility (ASF) located at the University of Alaska, Fairbanks. Calibration coefficients (available beginning October 1998) for calculation of normalized radar cross section (RCS) for RADARSAT ScanSAR imagery, as well as calibration and mapping techniques and software

have been supplied by the ASF and used in the data processing.

In support of the Alaska SAR Demonstration project, two wind retrieval models have been developed by The Johns Hopkins University Applied Physics Laboratory (APL procedure) and ERIM International Inc. (ERIM procedure). The APL model estimates the SAR wind direction from temporally coincident meteorological model output, and thus SAR wind direction accuracy depends directly on model wind accuracy. A SAR wind speed image is then estimated from the SAR RCS measurements using the CMOD4 wind speed algorithm modified for HH polarization. The ERIM procedure first estimates the wind direction from wind-aligned features in the SAR image (e.g., wind rows, convective cells, surfactants, etc.) and then estimates the wind speed in a manner similar to the APL approach, although with different radar cross section models. The wind vector retrieved from the ERIM procedure has 180 degree wind direction ambiguity.

2. RADARSAT SAR CALIBRATION

The retrieval of ocean surface wind from SAR imagery is dependent upon the knowledge of RCS obtained from calibrated imagery. Since late 1998, RADARSAT ScanSAR Wide B SAR imagery processed at the ASF has been certified as calibrated. Calibrated imagery provided in the Committee on Earth Observation Satellites (CEOS) SAR data format is accompanied by a leader file containing the appropriate coefficients for converting the digital value in the image into RCS using the following equation (for data processed at ASF):

$$\sigma_0 = a_2(d^2 - a_1 n(\theta)) + a_3 \quad (1)$$

where $a_1=21947.9$, $a_2=1.1026 \times 10^{-5}$, and $a_3 = 0.00000$ are typical values. The quantity d is the digital value in the image, and $n(\theta)$ is a noise value represented by a lookup table that describes the noise floor as a function of ground range (values are typically in the range $0.0093 < n < 0.2417$). The noise floor information in the leader

file, however, is not correct. The effect of an incorrect noise floor in the leader file is shown in Figure 1. The wind speed image in the left panel was derived from SAR data calibrated to RCS using the leader file information. Using wind directions obtained from the NOGAPS model, a wind speed at each pixel location was computed. The right panel was computed the same way except that the RCS values came from the ASF calibrate program, software made available on the ASF web site (<http://www.images.alaska.edu/software.html>). The overall structure and the range of the wind speeds are the same in the two images. However, at the very lowest wind speeds, the left image exhibits a rather unrealistically large region of zero wind speed.

Although the calibration scheme using the leader file produces reasonable cross sections values, the difference in the noise floor guarantees systematic problems, particularly at low wind speeds. For the Alaska SAR Demonstration, both the APL and ERIM procedures incorporate the ASF calibration software rather than using the leader file in order to produce accurately calibrated images for wind calculation.

Most of the SAR data to be used in the Alaska SAR Demonstration are ScanSAR data geocoded at the ASF to polar stereographic projection with a standard latitude of 70°N and a prime longitude of 45°W. Using Earth location information found in the map projection data record of the ASF SAR leader file, latitude and longitude are calculated for any pixel in the image using software obtained from ASF and incorporated into the wind processing modules.

3. SAR DERIVED OCEAN SURFACE WIND

Measurement of ocean surface winds from satellite scatterometer data is now quasi-operational. Routine availability of ERS-1/2 C-band scatterometer and the ADEOS Ku-band scatterometer data have fostered the development of mature algorithms for derivation of wind speed and direction from this type of data. But SAR instruments also have the potential for wind measurement. Like scatterometers, a SAR instrument measures variations in radar backscatter from the wind-roughened ocean, variations that are a function of wind speed and direction. Unlike scatterometers, SAR instruments only have one azimuth viewing angle, so wind direction must be obtained using a technique that differs from the multiple-azimuth measurement algorithm in use with modern scatterometers. An independent estimate of local wind direction, either from model output or from another source, is required for accurate wind measurement. Under the right

conditions, wind-aligned patterns in the SAR data itself can be used to infer wind direction with 180-degree ambiguity [1]. SAR wind measurements have the advantage of being at very high spatial resolution (in the range of 300 m to 1 km as opposed to the normal scatterometer resolution of 25-50 km) and can be made right up to the coast or in bays and estuaries without suffering from the land contamination evident in scatterometers and passive microwave radiometers. Two SAR wind products are being generated for the Alaska SAR Demonstration. Both products will be evaluated as to their utility to operational weather forecast and analysis activities; and ways of combining both algorithms to improve the wind product will be investigated.

3.1 APL WIND ALGORITHM

The APL wind algorithm is based on the CMOD4 algorithm [4,8]. The relationship between wind speed and direction and RCS is given by the CMOD4 algorithm as:

$$\sigma_0^V = a(\theta)f(U)^{\gamma}[1+b(\theta)\cos\phi+c(\theta,U)\cos 2\phi]^{1.6} \quad (2)$$

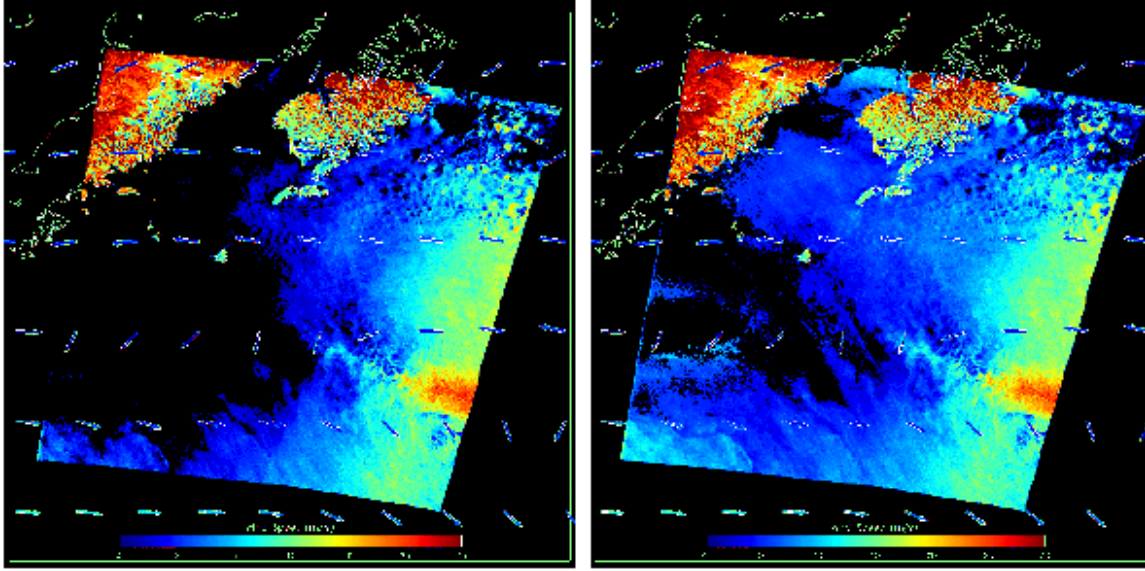
where σ_0^V is the vertical RCS, U is the wind speed, θ is the local incidence angle, and ϕ is the angle between the SAR look direction and the local wind direction. This model was developed for the ERS-1 C-band vertically polarized scatterometer (C-VV). Since RADARSAT SAR imagery is acquired at C-band horizontal polarization (C-HH), the CMOD4 algorithm needs to be modified for use with RADARSAT. The following relation between RCS for C-VV and C-HH has been derived at JHU/APL [5]:

$$\sigma_0^H = \sigma_0^V \frac{(1+\alpha \tan^2 \theta)^2}{(1+2 \tan^2 \theta)^2} \quad (3)$$

where α is a parameter that is still an area of research, and has been empirically estimated to be 0.6 [2,5]. Note that for an incidence angle of 0, $\theta = 0$, $\sigma_0^H = \sigma_0^V$.

Figure 1 is an example of the APL wind image product derived from SAR data using Equations (2) and (3). The RADARSAT ScanSAR Wide B geocoded polar stereographic image data are averaged to 400 m pixels and calibrated to RCS. Wind direction is obtained from the 1° × 1° latitude/longitude grid NOGAPS (Naval Operational Global Atmospheric Prediction System) meteorological model analysis or forecast closest in time to the SAR image. The model wind directions are interpolated down to the 400 m SAR pixels with a bilinear

Figure 1. Sample wind image derived from APL wind algorithm. Left image was calibrated with data from leader file. Right image was calibrated with ASF software. Image is of the Gulf of Alaska with Kodiak Island in the top center of the image. North is up.



interpolation scheme. Equations (2) and (3) are used to prepare a lookup table that returns wind speed output given RCS horizontal polarization input. In Figure 1, SAR wind speed is shown in the image color value. Arrows in the wind image are wind vectors from the NOGAPS model [2].

3.2 ERIM WIND ALGORITHM

The ERIM ocean surface wind product is derived with a different approach to the problem of measuring winds from SAR. SAR images over the ocean contain signatures of atmospheric effects due to the local changes to surface wind speed and direction. These signatures are often elongated in the general direction of the local wind. Examples are wind rows and island wind shadows [1]. In the ERIM procedure, land is first masked out of a RADARSAT SAR image using a coastline map (a 2 km uncertainty is added to take care of navigation errors). Multiple spatial frequency spectra are generated within a 48 km region of the SAR image with Fast Fourier Transforms. These spectra are then averaged to form a smooth spectrum. Next, the elongation direction of the spectral energy over large scales (3-20 km) is calculated with the elongation direction determined in two ways: (1) by fitting a quadratic polynomial to the spectrum and calculating the direction of smallest curvature, and (2) by finding the spectrum peak value. The wind direction is rotated 90 degrees from this elongation direction. This procedure is repeated with slightly overlapping regions

to form a 32 km grid of wind directions with 180-degree ambiguity. For each 48 km region used to estimate a wind direction, the average RCS of the region is also calculated, and then a 3 x 3 smoothing operation is applied to the wind directions where each direction is replaced by the weighted average of nine wind directions surrounding it with the average RCS values providing the weights. Finally, for each grid location the wind speed is estimated as follows. Given some model for the RADARSAT C-HH σ_0^H , wind speeds from 1 m/s to 30 m/s every 0.2 m/s are put into the model along with the estimated wind direction to generate an estimated σ_0^H . The wind speed that generated the estimated σ_0^H closest to the actual σ_0^H is chosen as the wind speed for that grid location. Currently, three RADARSAT C-HH σ_0^H models are being evaluated. The first is the same as in Equation (3) above. The second is similar to Equation (3), but where the CMOD4 scale factor is a cubic polynomial in $\tan(\theta)$ and the polynomial coefficients are empirically derived so that

$$\sigma_0^H = \sigma_0^V (\alpha_3 \tan^3 \theta_i + \alpha_2 \tan^2 \theta_i + \alpha_1 \tan \theta_i + \alpha_0) \quad (4)$$

The third model is a two-scale model with hydrodynamic effects that is being investigated to obtain a refined C-HH σ_0^H model [3,6,7]. This is defined as

$$\sigma_0^H = \iint \sigma_b(s_u, s_c) [1 + s(u)h(s_u, s_c)] \rho(s_u, s_c) ds_u ds_c \quad (5)$$

where s_u, s_c are the wave height slopes in the upwind and crosswind directions respectively, $\sigma_b(s_u, s_c)$ is the tilted bragg RCS for an ocean surface with the given slopes, $s(u)h(s_u, s_c)$ represents a modulation to the bragg RCS due to hydrodynamic effects (with u representing wind speed, $s(u)$ a scale factor based on wind speed, and $h(s_u, s_c)$ a linearization of the hydrodynamic effects in upwind and crosswind slopes), and $\rho(s_u, s_c)$ is the probability that a facet with slopes s_u and s_c occurs on the ocean surface.

Since the underlying RADARSAT C-HH σ_0^H model is so important to the final wind vector product, a study is underway to validate the different models and perhaps combine them into a final version. Figure 2 shows a plot of each model versus actual RADARSAT C-HH values calculated from 46 samples where the wind information came from an *in situ* buoy and the radar cross section value came from an average of the calibrated RADARSAT image over a 1 km square around the buoy. In Figure 2, the Two-Scale Model refers to the model in Equation (5), the Empirical Scaling Model refers to Equation (4), and the bragg Scaling Model refers to Equation (3). The normalized root mean square error (NRMSE in the figure) represents the mean square of the error between the model and RADARSAT RCS values (calculated in energy, not dB) normalized by the total energy in the RADARSAT values. Note that the NRMSE values are between 0.35 to 0.39 with the two-scale model performing slightly better than the other two. However it should be noted that the two-scale model takes much longer to calculate than the other two models. Work is ongoing to finalize these models.

Figure 2. Comparison of the various RADARSAT C-HH radar cross section models to RCS values calculated from calibrated RADARSAT images.

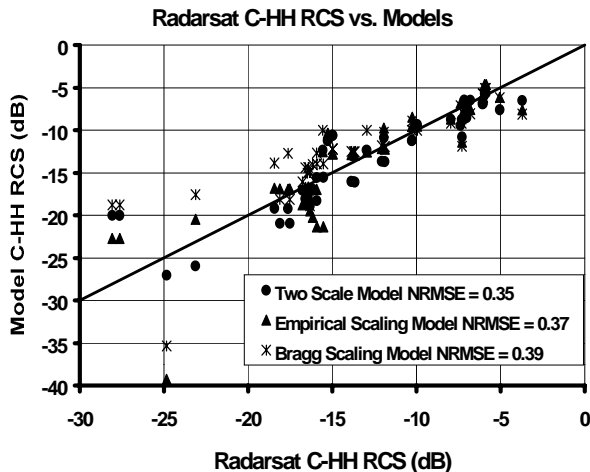
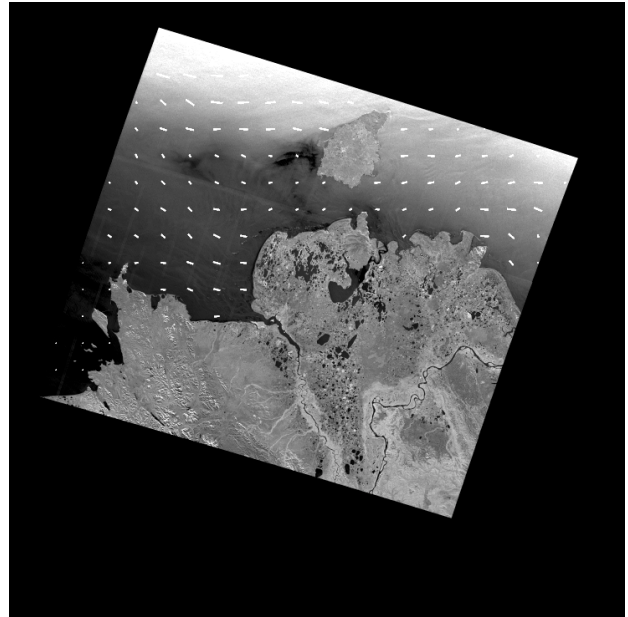


Figure 3 is an illustration of the ERIM wind product. The actual product is a text file of wind speed and direction for each grid point. In Figure 3, the vectors have been plotted on the SAR image from which they were derived to visualize the result.

Figure 3. A sample ERIM wind vector product derived from the SAR image. Image is of the Bering Sea. Nunivak Island is at the top center of the image. North is to the lower left portion of the image. SAR image Copyright, Canadian Space Agency, 1999.



4. VALIDATION OF SAR WIND PRODUCTS

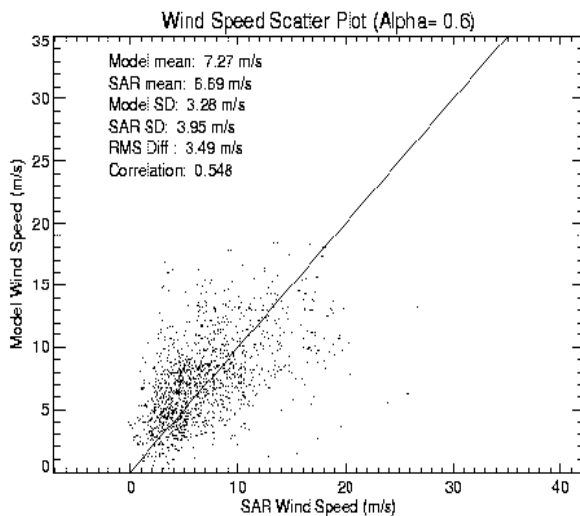
A validation system has been developed such that for each calibrated SAR image containing a meteorological buoy, the simultaneous buoy measurements (± 30 minutes) for the SAR image are extracted. A SAR wind image and SAR wind vectors are then processed from the calibrated SAR image. Finally, the wind measurements calculated from the SAR image at the buoy locations are extracted together with the buoy report to form a matchup file. In addition, the APL SAR winds are compared with the Navy NOGAPS meteorological model winds.

4.1 VALIDATION OF APL WIND IMAGES USING THE NAVY NOGAPS NUMERICAL MODEL

As a preliminary validation of the APL wind product, a comparison is made with the NOGAPS model winds that provide the directional information for the APL

model. The NOGAPS wind speeds are compared with the SAR wind speeds to detect any systematic errors. Figure 4 is a scatter plot of model wind speed derived from approximately 200 ScanSAR Wide B images versus SAR wind speed. The RMS difference is 3.49 m/s, with the mean of the SAR winds being 0.58 m/s lower than the model winds.

Figure 4. Comparison between the APL wind product with NOGAPS model wind.



4.2 VALIDATION OF THE ERIM WIND VECTORS USING NOAA MOORED METEOROLOGICAL BUOY DATA

Ten-meter winds measured by NOAA moored buoys are used as ground truth. The wind vector derived from RADARSAT SAR using the ERIM algorithms are compared with co-located buoy data. To date only ten matchup points have been used for wind direction comparisons whereas 46 have been used to estimate wind speed errors; wind direction validation utilizing the full 46 matches is currently underway. The wind direction comparison is given in Figure 5. Because of the 180 degree ambiguity in wind direction generated from the ERIM procedure, the error between the estimated and actual wind direction is always defined to be between ± 90 degrees. Thus the dashed lines in Figure 5 show the region within which the error must be by definition. One can see that the RMSE of the wind direction is 44 degrees with the peak algorithm and 33 degrees with the polynomial algorithm. In general we have found that the polynomial algorithm performs better than the peak algorithm, and routinely use that algorithm.

Figure 5. Comparison between wind direction derived from RADARSAT SAR using the ERIM algorithm and co-located NOAA moored buoy data.

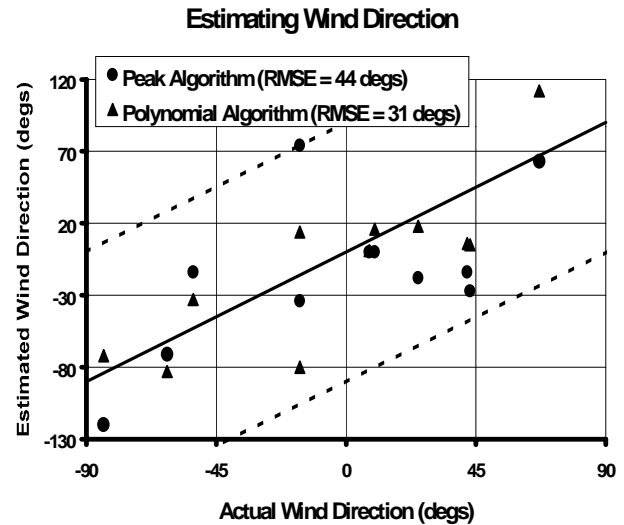
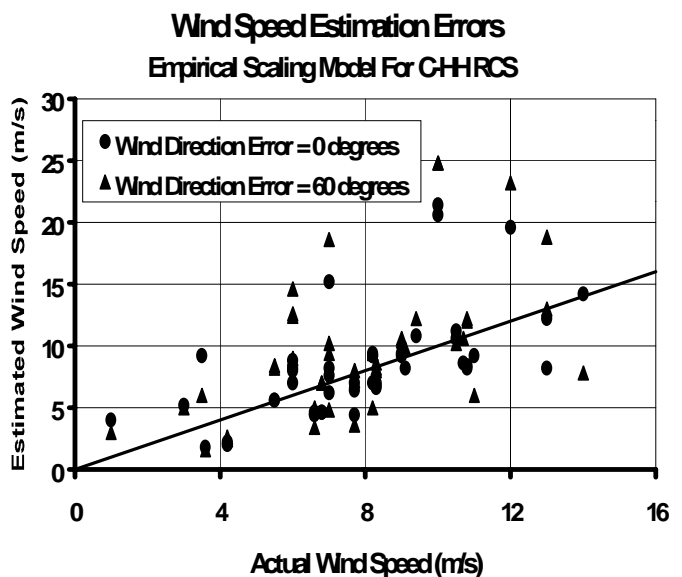


Figure 6 shows the resulting wind speed errors for the full 46 points where we have assumed an average wind direction error of 0 degrees and 60 degrees. For an average direction error of 0 degrees the wind speed RMSE was 3.41 m/s whereas for an average error of 60 degrees (which is much larger than expected) the wind speed RMSE was 4.85 m/s. A full validation for both wind direction and speed is underway, but we anticipate that the final wind speed RMSE will be close to 3.5 m/s.

Figure 6. Wind speed errors for the ERIM procedure for two different wind direction errors.



5. SUMMARY

Two wind retrieval procedures have been developed by The Johns Hopkins University Applied Physics Laboratory (APL procedure) and ERIM International Inc. (ERIM procedure) in support of the Alaska SAR Demonstration project. In this paper we give brief outlines of these models and some preliminary validation results. The APL procedure wind speed was compared with model wind measurements, and the RMSE in wind speed is about 3.49m/s. The ERIM model winds were compared with buoy winds and the RMS error in wind direction was between 31 and 44 degrees. The RMS error in wind speed was around 3.5 m/s.

6. ACKNOWLEDGEMENTS

Funding for the Alaska SAR Demonstration and research preceding the demonstration was provided by the NOAA/NESDIS Ocean Remote Sensing Program. RADARSAT data were provided under the NASA RADARSAT Applications Development and Research Opportunity (ADRO) Project 396.

7. REFERENCES

- [1] Fetterer, F, D. Gineris, and C. Wackerman, "Validating a wind Algorithm for ERS-1 SAR," *IEEE Trans. Geosci. and Remote Sens.*, 36, 479-492, 1998.
- [2] Monaldo, F., and R. Beal, "RADARSAT applications demonstration in the Gulf of Alaska," *Johns Hopkins University Applied Physics Laboratory Tech. Rep.*, SRO-99-07, PP. 1-18, 1999.
- [3] Romeiser, R. and V. Wismann, "An improved composite surface model for the radar backscattering cross section of the ocean surface 1. Theory of the model and optimization/validation by scatterometer data," *J. G. R.*, Vol. 102, No. C11, 25,237-25,250, 1997.
- [4] Stoffelen, A and D. L. T. Anderson, "Wind retrieval and ERS scatterometer radar backscatter measurements", *Adv. Space Res.*, 13, 53-60, 1993
- [5] Thompson, D. R., T. M. Elfouhaily, and B. Chapron, "Polarization ratio for microwave backscattering from the ocean surface at low to moderate incidence angles," *Proc. 1998 International Geoscience and Remote Sensing Symposium*, 1671-1673, 1998.
- [6] Valenzuela, G.R., "Theories for the interaction of electromagnetic and ocean waves – A review," *Boundary Layer Meteorol.*, 13, 61-85, 1978.
- [7] Wackerman, C., "Incorporating hydrodynamic effects into an analytic two-scale model to predict C-VV and C-HH observation," Unpublished, 1999.
- [8] Wismann, V., "A C-band scatterometer model derived from data obtained during the ERS-1 calibration/validation campaign," *Proc. First ERS-1 Symposium*, Cannes, 55-59, 1992.